Optimizing the environmentally friendly silica-cellulose aerogel composite for acoustic insulation material derived from newspaper and geothermal solid waste using a central composite design

by Ferry Hermawan

Submission date: 08-May-2023 11:33AM (UTC+0700)
Submission ID: 2087170593
File name: B-1.1-5_Optimizing_the_environmentally_friendly_silica-cel.pdf (3.02M)
Word count: 10577
Character count: 55171

Journal of Sol-Gel Science and Technology
https://doi.org/10.1007/s10971-022-05831-y

ORIGINAL PAPER: SOL-GEL AND HYBRID MATERIALS FOR ENERGY, ENVIRONMENT AND BUILDING APPLICATIONS

Optimizing the environmentally friendly silica-cellulose aerogel composite for acoustic insulation material derived from newspaper and geothermal solid waste using a central composite design

S. Silviana[1] · Ferry Hermawan[2] · Joshua Indracahya[1] · Dinda Ajeng Lestari Kusumawardhani[1] · Febio Dalanta[1]

Received: 22 December 2021 / Accepted: 26 April 2022

Abstract

This study aims to explore the combination of newspaper waste-derived cellulose and silica from geothermal solid waste to produce the silica-cellulose (Si-cellulose) aerogel as an enhanced sound insulation composite material. Cellulose was used as the matrix, while silica was applied as the impregnated particle to improve the characteristics and sound absorption ability of the composite. Subsequently, two datasets of central composite design (CCD) were used to generate the regression models the aerogel with the independent variables of cellulose and polyethylene glycol (PEG) concentrations as well as sound absorption coefficient (SAC) as the response. The generated regression models were evaluated using root-mean-square error (RMSE), analysis of variance (ANOVA), model adequacy, as well as diagnostics through normal plot of residuals, Cook's distance, leverage, and predicted vs. residuals plots. The generated response surface plots suggest that the maximum SAC will be achieved by maximizing the cellulose composition. Based on several characterizations, it was concluded that the embedded silica changed the physical, chemical, mechanical, and thermal stability of the fabricated composite evidenced by the enhanced acoustic insulation performance. Furthermore, the optimum point for Si-cellulose aerogel was found at cellulose and PEG compositions of 25%-w and 1.78%-w/v, respectively, which produced the predicted maximum SAC of 0.9896 with a desirability score of 0.967. Based on the validation experiment results, the actual SAC was 0.9992 with a difference from the predicted value of 0.96%, indicating that the generated model can precisely predict the actual SAC value for utilizing Si-cellulose as an acoustic insulation material.

✉ S. Silviana
silviana@che.undip.ac.id

[1] Department of Chemical Engineering, Faculty of Engineering, Diponegoro University, Semarang 50275, Indonesia

[2] Department of Civil Engineering, Faculty of Engineering, Diponegoro University, Semarang 50275, Indonesia

Published online: 13 May 2022

Graphical abstract

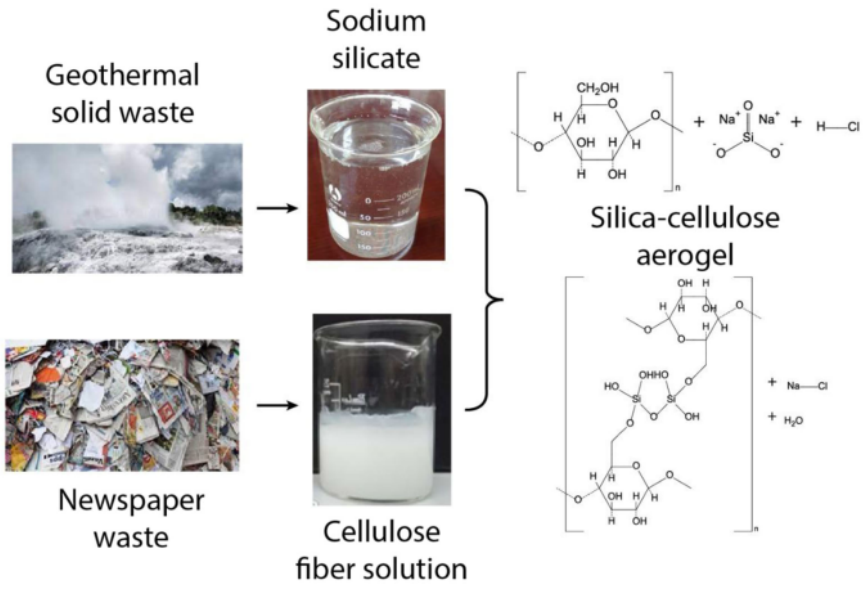

Keywords Optimization · Silica-cellulose aerogel · Central composite design · Acoustic insulation · Sound pollution.

Highlights

- Silica-cellulose aerogel derived from newspaper and geothermal solid waste was successfully synthesized as the acoustic insulation material.
- Optimization of the formulation was evaluated using central composite design.
- The impregnated silica was significantly enhanced the sound absorption ability and thermal stability of the composite.

1 Introduction

Noise has been considered for decades to be one of the big challenges on environmental activities and become the least maintained type of pollution. Continuous noise pollution can cause several health problems such as loss of hearing, as well as increasing psychological stress and blood pressure [1–3]. Meanwhile, acoustic insulations have been used to reduce noise pollution and the component material selection must be based on the quantity of sound transmitted, reflected, and absorbed [4, 5]. Several materials have been investigated for the preparation of acoustic insulators, such as ceramic, mineral wood, fiberglass, graphite, polypropylene, and polyester [6–8]. However, their high cost became the major obstacle to industrial-scale development [9, 10]. Different studies have been conducted on utilizing wastes as raw materials to synthesize acoustic insulation composites, including chicken feathers [11], sheep wool [12], silica aerogel [13], and cellulose [14].

One of the promising material sources is cellulose due to its proven ability to generate excellent acoustic insulation and widespread abundance. Moreover, it was found to have low density 0.017–0.029 g/cm,^{3} high porosity 98.2–98.9%, and a large specific surface area 296–412 m^2/g, suggesting a promising future acoustic insulator property [15]. Agricultural and forestry products have become well-known sources of cellulose [16–18]. However, the use of these resources contradicts environmental protection efforts. Various environmental problems might arise when cellulose is utilized excessively. Material flow analysis and life cycle assessment showed that cellulose fibers consumption in form of paper contributes significantly to climate change and urban air pollution [19]. These environmental implications are not only associated with paper consumption, but also with the production. Material processing, transport, filament manufacture, and byproducts disposal might contribute to environmental pollution as well as resource consumption such as freshwater and fossil fuels [20]. Dye-containing wastewater and noise pollution from paper and textile production also pose a risk of environmental damage, specifically to water and air (sound). Previous studies attempted to minimize this impact by degrading the

dye-containing wastewater [21–23] and reducing noise pollution [24, 25] using modified materials.

Cellulose can be generated from waste such as paper-related waste, for example, newspapers have a high cellulose content up to 45–55% after oxidizing and washing to remove the ink. However, the synthesis from recycled fibers has a lower mechanical strength than those made from new fibers. An improvement to the mechanical strength of cellulose from paper-related waste must be made [26]. One of the potential solutions is the impregnation with an inorganic material such as silica.

Silica has been widely used in many fields of application, such as zeolite synthesis, coating, slow-release fertilizer, drug delivery, catalysis, adsorbents, etc [27]. Its sources include rice husks, bamboo leaf [28, 29], straw, bagasse, corn cobs, [30], and geothermal solid waste [31–33] which has a high content up to 88.29% before purification and reaches 97% after acid leaching [34], but this potential has not been fully utilized [35]. The geothermal solid waste was used in this study as the silica source similar to that previously utilized in various applications [28, 36–40]. Several studies reported that silica has exquisite properties as a sound insulation material, including low thermal conductivity of 0.0010–0.050 W/mK, low bulk density 0.001–2.00 g/cc, large surface area 8.1–160 m^2/g, and high porosity 70–99% [31, 41–43], but it is also highly brittle and fragile [13]. Cellulose has been shown as a flexible and compressible material but has a relatively higher thermal conductivity than silica [44, 45]. Therefore, the idea of combining silica and cellulose to become silica-cellulose (Si-cellulose) aerogel as the sound insulation composite is promising and has gained significant attention [6, 13, 14, 46].

This study explores the combination of cellulose derived from newspaper and silica from geothermal solid waste to produce the Si-cellulose aerogel as an improved sound insulation composite material. Cellulose is used as the matrix of the composite, while silica will function as the impregnated particle to improve the mechanical strength, thermal stability, and sound absorption ability. Silica was impregnated with cellulose through the sol-gel method using sodium silicate and hydrochloric acid, then solidified using a freeze dryer to form Si-cellulose aerogel. This technique was used due to its cost-effectiveness rather than previously reported methods such as CCl_4 cold-plasma and methoxy trimethyl silane (MTMS) modification which needs plenty amount of chemicals and a longer processing time [13, 47]. In addition, two datasets of central composite design (CCD) with 13 runs were performed to comprehensively investigate the best formulation and evaluate the effect of variables on the fabricated cellulose and Si-cellulose aerogel.

Based on the literature, the investigation of Si-cellulose aerogel derived from newspaper and geothermal solid wastes as an acoustic insulation material using CCD experimental design has not been explored. Two datasets of CCD were used to generate the regression models of cellulose and Si-cellulose aerogel with the independent variables of cellulose and polyethylene glycol (PEG) concentrations, as well as sound absorption coefficient (SAC) as the response variable. The generated regression models were evaluated using analysis of variance (ANOVA), model adequacy, and diagnostics. They were used to generate the response surface plots for the optimization to predict the optimum point, while the validation experiment was conducted to validate the optimization results. Furthermore, several characterizations were applied to further evaluate the effect of the impregnated silica on Si-cellulose aerogels, including X-ray fluorescence (XRF) and energy dispersive x-ray (EDX) to reveal the silica content in the composites, scanning electron microscopy (SEM) to show the surface morphology of the composites, Brunauer-Emmet-Teller analysis (BET) for measuring the surface area and adsorption ability of the composites, Fourier-transform infrared (FTIR) analysis to inform the functional groups of the composites, as well as thermal gravimetric analysis (TGA) and differential scanning calorimetry (DSC) to provide the thermal characteristics. This study aims to synthesize Si-cellulose composite that is environmentally friendly and has promising acoustic insulation material ability from newspaper and geothermal solid wastes.

2 Materials and methods

2.1 Materials

Silica was directly supplied from the solid waste section of the geothermal powerplant owned by PT. Geo Dipa Energi, Wonosobo, Indonesia, while newspaper wastes as the source of cellulose were obtained from the waste center of the Department of Chemical Engineering, Diponegoro University, Semarang, Indonesia. Sulfuric acid (H_2SO_4, 98%), sodium hydroxide (NaOH, 98%), polyethylene glycol (PEG 400, 99%), ethanol (C_2H_5OH, 96%), ammonium hydroxide (NH_4OH, 25%), and hydrogen peroxide (H_2O_2, 32%) were purchased from Merck, Germany, while hydrochloric acid (HCl, 37%) was supplied by Mallinckrodt, Germany. All solutions were made using distilled (DI) water.

2.2 Methods

2.2.1 Preparation of purified silica from geothermal solid waste

The geothermal solid waste must be treated before the application as the silica source due to the high content of impurities, specifically the metal oxides. A total of 250 g

Table 1 The experimental results and the prediction values

Run	Cellulose (%-w)	PEG (%w/v)	Y_p (Prediction)	Y_a (Actual)	MSE
1	15.00	1.17	0.9341	0.9532	4.0900E-04
2	15.00	2.03	0.9697	0.9737	1.6209E-05
3	29.14	1.17	0.9879	0.9921	1.8035E-05
4	25.00	0.56	0.9824	0.9781	1.8137E-05
5	5.00	0.56	0.8348	0.8306	1.7412E-05
6	15.00	1.17	0.9341	0.9369	7.9072E-06
7	25.00	1.78	0.9886	0.9842	1.9519E-05
8	5.00	1.78	0.9430	0.9383	2.2391E-05
9	15.00	1.17	0.9341	0.9151	3.0010E-04
10	15.00	0.30	0.9653	0.9698	2.0647E-05
11	0.86	1.17	0.8264	0.8302	1.4661E-05
12	15.00	1.17	0.9341	0.9308	1.0811E-05
13	15.00	1.17	0.9341	0.9345	1.6970E-07
RMSE					3.4000E-04

geothermal solid waste was carefully dried using oven at 110 °C until constant weight, then it was crushed into a finer powder. Furthermore, the leaching treatment was conducted to remove the metal oxides from the sample. This was carried out using previously reported methods with some modifications [48]. A total of 125 g geothermal solid waste was immersed and constantly mixed in 500 mL of 20% H_2SO_4 at 110 °C for 105 min. Subsequently, the mixture was repeatedly washed and rinsed using DI water until a neutral pH was achieved. It was then filtered using filter paper to get the solid from the mixture using a vacuum filter, then the solid was dried using oven at 110 °C until constant weight.

2.2.2 Preparation of sodium silicate

The next step in the purification process was the preparation of sodium silicate which referred to previously reported methods [48]. A total of 100 g purified silica was constantly mixed in 600 mL of 2 N NaOH solution at 95 °C for 1 h. The silica was gradually dissolved in NaOH solution leaving the impurities in the solid form. Subsequently, the generated solution was filtered, and the filtrate was carefully collected and denoted as sodium silicate.

2.2.3 Preparation of cellulose fiber solution

This procedure was applied to get the cellulose fiber from the newspaper waste by referring to the previous study with several modifications [49]. A total of 100 g newspaper waste was cut into pieces as small as possible and then constantly mixed into a solution containing 5% NaOH for 3 h and was left overnight. Furthermore, the mixture was filtered, while the solid was further mixed in a solution containing 32% H_2O_2 and heated at 50 °C for 2 h. The mixture was separated using a vacuum filter followed by repeated washing and rinsing until a neutral pH was achieved. The solid product from filtration was the cellulose fiber, and it was carefully collected. Subsequently, the cellulose fiber solutions were made by dispersing with DI water in 10 mL on a basis using an ultrasonic homogenizer with cellulose variations of 0.86; 5.00; 15.00; 25.00; and 29.14%-w.

2.2.4 Preparation of cellulose aerogel

This procedure was conducted by applying CCD with 13 runs using Design-Expert software v.8.0.6 based on previously reported methods [50]. The experimental design is summarized in Table 1, at the beginning, the prepared cellulose fiber variations of 0.86; 5.00; 15.00; 25.00; and 29.14%-w was added into the solution containing 10% NaOH and PEG 400 that varied with 0.3; 0.56; 1.17; 1.78; 2.03%-w/v. The mixtures were constantly stirred for 5 h at room temperature, then 2 N of HCl was added and was filtered to separate the solid which was immersed in DI water and ethanol respectively for 6 h. This procedure was repeated three times, and re-filtered, then the solid was dried in a freeze dryer to form the cellulose aerogel.

2.2.5 Preparation of Si-cellulose aerogel

This procedure was conducted based on a previously reported method [47] by applying a CCD with 13 runs using Design-Expert software v.8.0.6. The experimental design is summarized in Table 4, it was conducted to investigate the effect of impregnated cellulose aerogel with silica on acoustic insulation ability. The cellulose aerogel obtained from the freeze-drying process was immersed in the sodium silicate solution and constantly mixed for 6 h at room temperature.

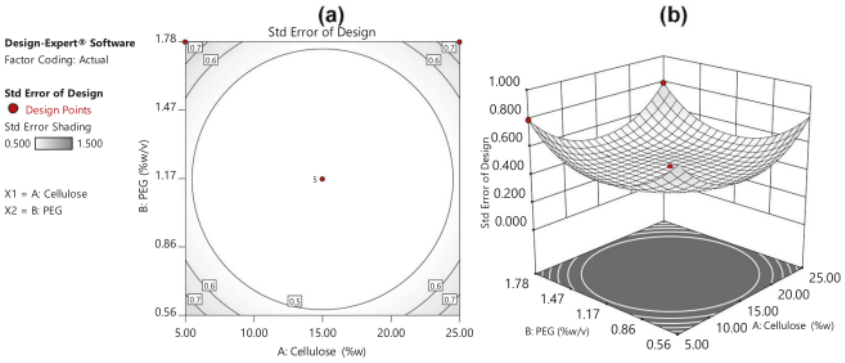

Fig. 1 Evaluation of the standard error of design for the experimental design for the cellulose aerogel. **a** Contour plot of the standard error of design and **b** surface plot of the standard error of design

The mixture was added with 2 N HCl dropwise until pH = 2 was achieved, then NH_4OH was added and left for 3 days for the aging process. The product formed was proceeded through a freeze dryer to get the Si-cellulose aerogel.

2.2.6 Determination of acoustic insulation ability through sound absorption coefficient (SAC)

The acoustic insulation ability of cellulose and Si-cellulose aerogel were conducted by measuring their SAC. A sound generator with certain intensity was used to produce the signal, and a sound meter (Sound Level Meter, Lutron SL-4011, Taiwan) was used to measure the absorption coefficients. SAC is represented by Eq. 1 [51]:

$$\alpha = 1 - \frac{I_R}{I_I} \tag{1}$$

Where α is SAC, I_R is absorbed and/or reflected sound (W/m^2), and I_I is the radiated sound (W/m^2). SAC values vary, ranging from 0 to 1, a value of 0 indicates no absorption, while 1 indicates perfect sound absorption. In the case of $\alpha = 0$, sound completely passed through the material, while $\alpha = 1$ indicates that it is almost completely absorbed and only a little amount is reflected by the material.

2.2.7 Product characterizations

The morphology and the surface elemental composition of Si-cellulose aerogel were observed using scanning electron microscopy coupled with an energy dispersive x-ray (SEM-EDX, Thermo Fischer Scientific, USA). Moreover, the chemical composition was investigated using x-ray fluorescence (XRF, Shimadzu, Japan), while the functional groups were observed using a Fourier-transform infrared (FTIR, IRPrestige21 Shimadzu, Japan). The thermal behavior of Si-cellulose was analyzed using a thermogravimetric analysis (TGA) coupled with differential scanning calorimetry (DSC) (TGA/DSC, Linseis STA 1600 Premium Series, USA), while the specific surface area was determined using a Brunauer-Emmet-Teller analysis (BET, Quantachrome Instruments, Switzerland).

3 Results and discussion

3.1 Statistical study of cellulose aerogel as the acoustic insulation material

3.1.1 Model development

The developed empirical model was used to explain the interaction between the independent variables namely cellulose and PEG as well as their effects on the response variable. Meanwhile, it is important to check the standard error of design (SED) to evaluate the prediction precision, which was CCD with 13 experimental runs. Figure 1 shows the contour and surface plots of the SED that is being evaluated. The darker shading represents a higher error, while the lighter shading depicts the lower error in the design space. Based on the figure, the measured SEDs are relatively low, with values ranging from 0.5 to 0.7. Therefore, this particular design can be used to promote an accurate prediction model [52].

The experimental results and their comparison with the prediction value are listed in Table 1. The experimental result was also statistically evaluated using the regression equation as the developed equation is mathematically expressed in Eq. (2).

$$SAC = 0.9431 + 0.0571A + 0.0016B + 0.0255AB + 0.0135A^2 + 0.0166B^2 + 0.0271A^2B - 0.0088AB^2 \tag{2}$$

Where SAC represents the sound absorption coefficient, while A and B represent the cellulose (%-w) and PEG content (%-w/v), respectively.

Table 2 Summary of ANOVA result and model adequacy indicators for the effects of cellulose and PEG concentrations upon the SAC

Source	Sum of squares	Degree of freedom	Mean square	*F*-value	*p*-value	Results
Model	0.0320	7	0.0046	25.42	0.0013	significant
A- Cellulose	0.0130	1	0.0130	72.47	0.0004	significant
B- PEG	9.741E-06	1	9.741E-06	0.0541	0.8253	not significant
AB	0.0026	1	0.0026	14.50	0.0125	significant
A^2	0.0013	1	0.0013	7.04	0.0453	significant
B^2	0.0019	1	0.0019	10.73	0.0221	significant
A^2B	0.0015	1	0.0015	8.17	0.0354	significant
AB^2	0.0002	1	0.0002	0.8685	0.3942	not significant
Residual	0.0009	5	0.0002			
Lack of fit	0.0002	1	0.0002	0.8090	0.4193	not significant
Pure error	0.0007	4	0.0002			
Cor total	0.0329	12				
Fit statistics						
R^2	Adjusted R^2	Predicted R^2	Adequate Precision	Std. Deviation	Mean	C.V.%
0.9727	0.9344	0.6732	15.47	0.0134	0.9360	1.43

The developed regression equation follows a cubic model which was evaluated by calculating the mean square error (MSE) and the root-mean-square error (RMSE) between the predicted and actual values, as completely summarized in Table 1. Based on the results, the errors between the predicted and actual experiment values are relatively low, indicating that the model can precisely predict the response. The calculated RMSE for this result was 3.40E-04, the lower value, the higher the precision of the developed model in predicting the response.

3.1.2 Study of analysis of variance (ANOVA), model adequacy indicators, and diagnostics

ANOVA was used to evaluate the significance of the developed model either in single or interactive terms. Table 2 shows the summary of ANOVA and the model adequacy indicators for the effects of cellulose and PEG concentrations on SAC. The significance of the parameters was determined using the *F* and *p*-value. The result is significant when the *F*-value is higher and the *p*-value is lower than 0.05 at 95% level of confidence [53]. Based on the ANOVA result, the cubic model performed a significant prediction with a *p*-value of 0.0013, while the single interaction of cellulose in the composite produced a significant effect with a *p*-value of 0.0004. In contrast, single interaction of PEG showed an insignificant effect in the composite with a *p*-value of 0.8253. The interaction between cellulose and PEG (AB) indicated a significant effect along with other interactions of A^2, B^2, and A^2B, while the AB^2 effect was insignificant with a *p*-value of 0.3942. The developed model also had an insignificant lack of fit demonstrated by the *p*-value of 0.4193. Hence, from this ANOVA analysis, almost all of the interactions showing significant effects had insignificant lack of fit values, signaling that the model is acceptable.

The developed model was also evaluated through the coefficient of determination (R^2), adj-R^2, pred-R^2, adequate precision, standard deviation, mean, and CV%. The result of the coefficient determination was desirable with a value of 0.9727 indicating a good fit for the model. Both the adj-R^2 (0.9344) and pred-R^2 (0.6732) were also in high precision of fit, meaning the quality and significance of the model. To verify the quality of the model in the actual experimental data, the adequacy precision was found to be 15.47, which is acceptable because it is above the minimum value of 4. Additionally, the standard deviation of the model was measured to be 0.0134, which is relatively low and acceptable. The mean value was found to be 0.9360, while CV% was 1.43% which represents high data reliability. The ANOVA and adequacy parameter authenticates the developed SAC model with cellulose aerogel as the material and suggests further diagnostics.

The diagnostics were analyzed to check whether the errors of the developed model are independently or identically distributed. This was carried out using the normal plot of residuals, cook's distance, leverage plot, and residuals vs. predicted plot, as shown in Fig. 2. Furthermore, Fig. 2a shows that the externally studentized residuals were well fitted on the normal plotline suggesting that the model is adequate. The Cook's distance represents the effect of a single run on the developed model that measures the changes in model parameters after replacing a particular actual run. Figure 2b shows that two

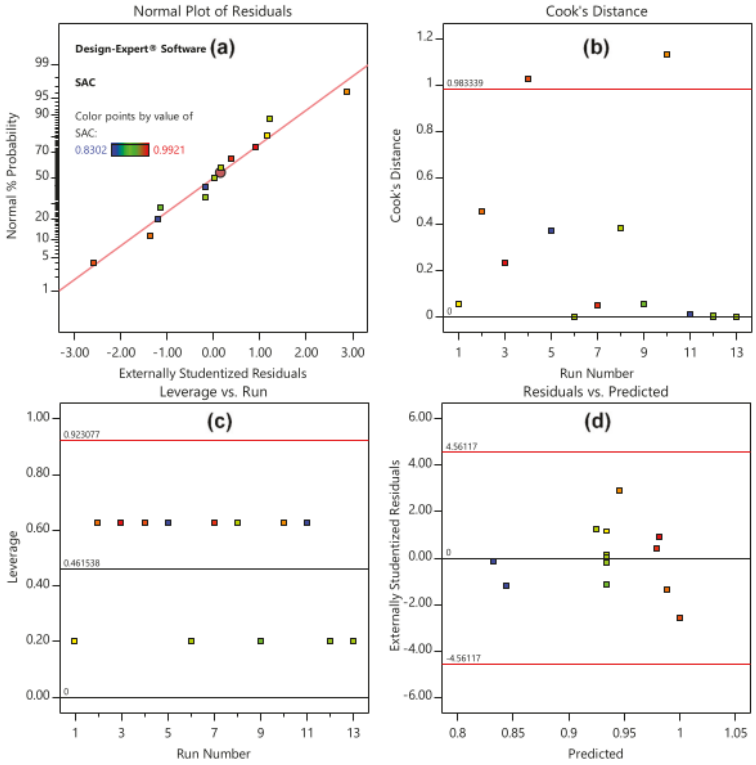

Fig. 2 Plotting for diagnostics of the developed model. **a** Normal plot of externally studentized residuals, **b** Cook's distance, **c** leverage plot vs. the run, and **d** residuals vs. predicted plot

experimental runs fall outside Cook's line, which is probably the spot of the insignificant parameters. Figure 2c, d present the leverage and residuals vs. predicted plots that show the uniform distribution of the data on the developed response model. This uniform distribution indicates the good adequacy of the model to predict the response in the design space. Therefore, it can be reasonably stated that the model is adequate and can be used to navigate the response data.

3.1.3 Response surface analysis and optimization

The influences of cellulose and PEG on SAC values can be estimated by assessing the response surface plot generated from the regression equation. Figure 3a shows the contour plot, and Fig. 3b depicts the response surface plot representing the influence of cellulose and PEG concentration on the SAC. The SAC values varied, ranging from 0.8302 to 0.9921. Based on these figures, it can be seen the blue region represents the lower SAC, whereas the red region represents the higher SAC. The higher SAC was established in a higher concentration of cellulose and PEG, while the lower SAC presented in a lower concentration of cellulose and PEG. The changing concentration of cellulose and PEG have significantly influenced the sound absorption of the composite. However, it can also be seen that cellulose plays a more dominant role in sound absorption to result in a higher SAC. At a lower concentration of PEG, the cellulose alone can still generate a higher SAC value, but at a lower concentration of cellulose, the measured SAC values were low. Therefore, it is obviously clear that cellulose plays a key role in sound absorption.

The information from response surface plots is essential to perform an optimization. The primary goal was to find the formulation that generated the highest SAC value, hence, the optimization was targeted to (i) maximize the SAC value, (ii) maximize the utilization of cellulose, and (iii) select the PEG concentration. Furthermore, the optimization was conducted by applying the desirability parameter, which considers all targets into a single desirability score. Figure 4a shows the contour plot, Fig. 4b represents the surface plot of the SAC predicted value from optimization, while 4(c) shows the contour plot. Figure 4d presents the surface plot of the desirability score, while Fig. 4e represents the Ramp's diagrams of the optimization result showing that at 25%-w of cellulose and 1.78%-w/v of PEG, a SAC value of 0.9886 can be achieved with a desirability score of 0.9891.

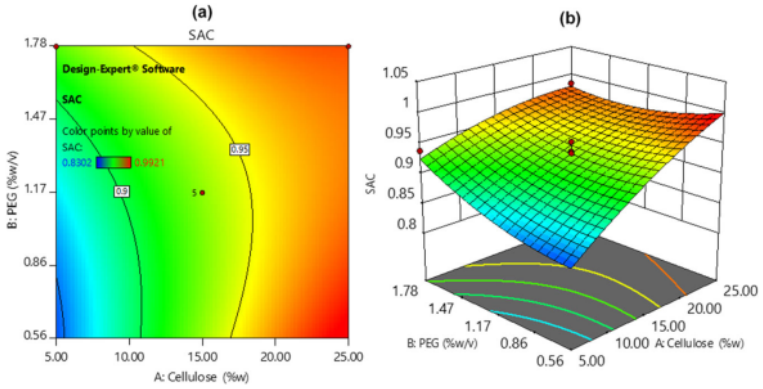

Fig. 3 Plotting of response surface from the regression equation. **a** Contour plot and **b** surface plot 3D for the effects of cellulose and PEG on the SAC

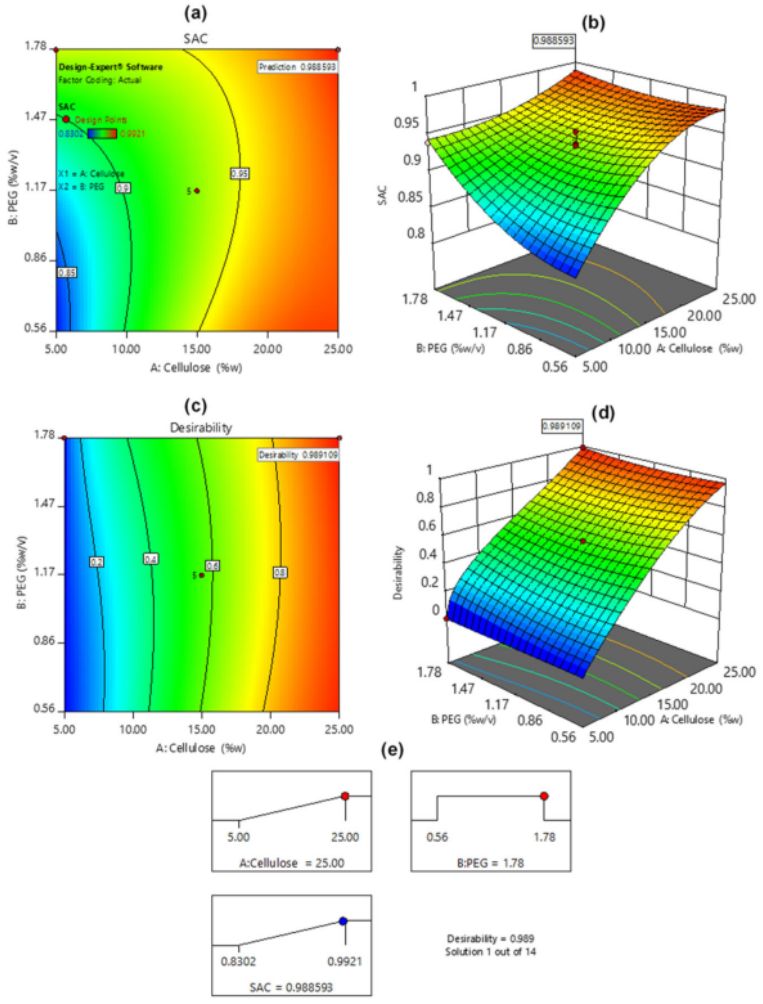

Fig. 4 Plotting of the optimization result for the cellulose aerogel. **a** Contour plot of predicted SAC, **b** surface plot of predicted SAC, **c** contour plot of estimated desirability, **d** surface plot of estimated desirability, and **e** Ramp diagram

Table 3 RMSE estimation of the developed model

Run	Si-Cellulose (%w)	PEG (%w/v)	Y_p (Prediction)	Y_a (Actual)	MSE
1	15.00	1.17	0.9473	0.9614	3.0340E-04
2	15.00	2.03	0.9974	0.9991	3.0207E-06
3	29.14	1.17	0.9910	0.9931	1.1866E-06
4	25.00	0.56	0.9808	0.9787	7.2867E-06
5	5.00	0.56	0.8695	0.8676	3.6977E-06
6	15.00	1.17	0.9473	0.9350	8.9853E-05
7	25.00	1.78	0.9896	0.9875	2.9307E-05
8	5.00	1.78	0.9432	0.9408	2.3808E-05
9	15.00	1.17	0.9473	0.9396	5.8966E-05
10	15.00	0.30	0.9457	0.9479	6.0021E-04
11	0.86	1.17	0.8493	0.8511	3.3059E-06
12	15.00	1.17	0.9473	0.9512	1.5373E-05
13	15.00	1.17	0.9473	0.9487	2.0189E-06
RMSE					4.2000E-05

Table 4 Summary of ANOVA result and model adequacy indicators for the effects of Si-cellulose and PEG concentrations on the SAC

Source	Sum of squares	Degree of freedom	Mean square	*F*-value	*p*-value	Results
Model	0.0230	7	0.0033	35.61	0.0006	significant
A- Si-Cellulose	0.0100	1	0.0100	108.89	0.0001	significant
B- PEG	0.0013	1	0.0013	14.41	0.0127	significant
AB	0.0011	1	0.0011	11.43	0.0196	significant
A^2	0.0013	1	0.0013	13.88	0.0136	significant
B^2	0.0010	1	0.0010	11.07	0.0209	significant
A^2B	0.0000	1	0.0000	0.1273	0.7358	not significant
AB^2	0.0002	1	0.0002	2.50	0.1750	not significant
Residual	0.0005	5	0.0001			
Lack of fit	0.0000	1	0.0000	0.3270	0.5981	not significant
Pure error	0.0004	4	0.0001			
Cor total	0.0235	12				
Fit statistics						
R^2	Adjusted R^2	Predicted R^2	Adequate Precision	Std. Deviation	Mean	C.V.%
0.9803	0.9528	0.8775	19.65	0.0096	0.9463	1.01

3.2 Statistical study of cellulose aerogel impregnated with silica as the acoustic insulation material

A statistical study was conducted on further modification of cellulose aerogel with silica impregnation (Si-cellulose) to enhance the sound absorption performance. Meanwhile, a similar method of investigation with the previous discussion was performed to show the comparison between cellulose and Si-cellulose aerogel for acoustic insulation material.

3.2.1 Model development

CCD with 13 experimental runs was employed to statistically assessed the effect of silica impregnated cellulose and PEG concentration on SAC to find the optimum formulation. The experimental result was evaluated using a regression equation shown in Eq. (3).

$$SAC = 0.9473 + 0.0501A + 0.0182B + 0.0162AB + 0.0136A^2 + 0.0121B^2 + 0.0024A^2B - 0.0107AB^2 \quad (3)$$

Where SAC, A and B represent the sound absorption coefficient, Si-cellulose (%w) and PEG content (%w/v), respectively.

This generated model follows a cubic model, while the experimental results and their comparison with the prediction value are summarized in Table 3. To evaluate this model, the errors were determined by calculating MSE and RMSE between the predicted and actual values. Table 3 shows that the MSEs were relatively small, the lowest namely 1.1866E-06 was found with 29.14%-w of Si-cellulose and 1.17%-w/v of PEG, showing 0.991 and 0.9931 of the predicted and actual SAC. In comparison, the highest namely 6.0021E-04 was found with 15%-w and 0.3%-w/v, showing 0.9457 and 0.9479 of the predicted and actual SAC, respectively. It was also found that the RMSE was 4.200E-05, this was lower than the cellulose and PEG model, which was 3.400E-04. This implies that the Si-cellulose and PEG model provides a better prediction of SAC than cellulose and PEG.

3.2.2 Study of analysis of variance (ANOVA), model adequacy indicators, and diagnostics

ANOVA was employed to assess the significance of the model and its terms, Table 4 shows the results and the model adequacy indicators for the effects of Si-cellulose and PEG concentrations on SAC. Based on the ANOVA result, the regression model had a significant effect with a *p*-value of 0.0006. Both single interactions of Si-cellulose and PEG had significant impacts with *p*-values of 0.0001 as well as 0.0127 for cellulose and PEG, respectively. In previous results (Table 2), a single effect of PEG was found to be insignificant with

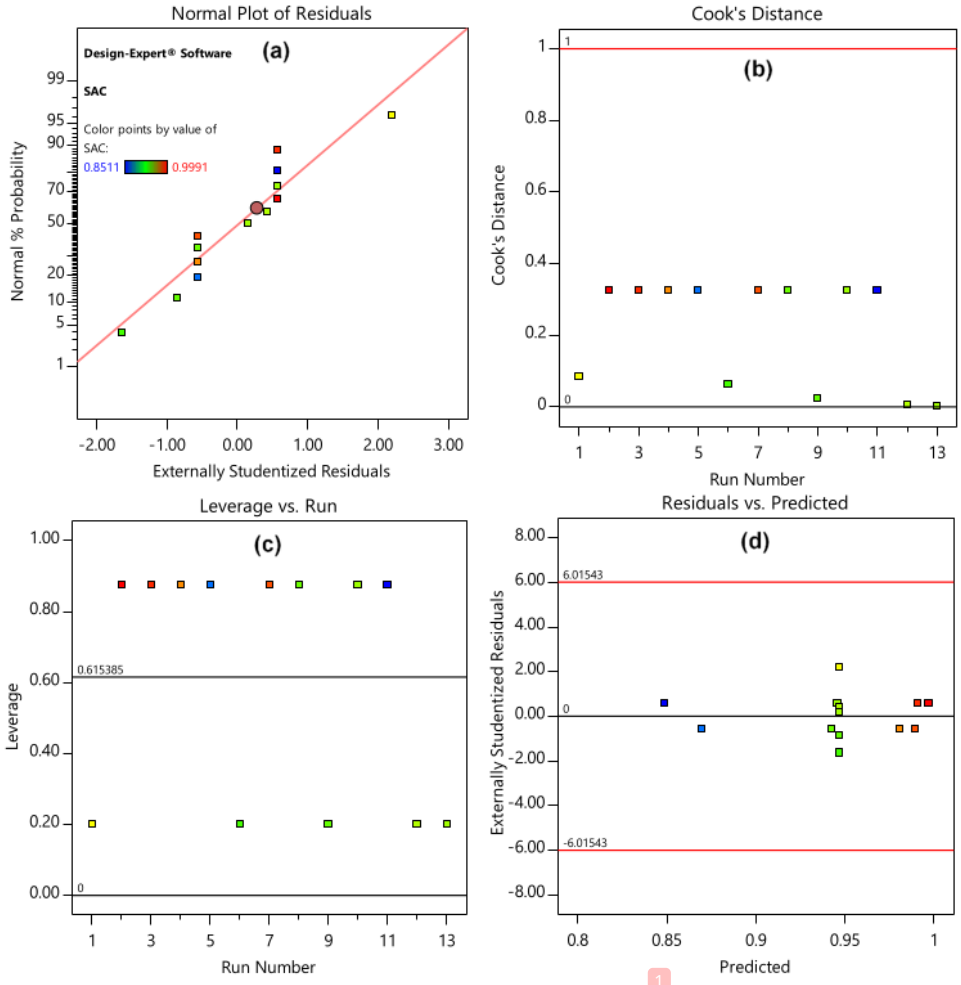

Fig. 5 Plotting for diagnostics of the developed model for Si-cellulose and PEG on SAC. **a** Normal plot of externally studentized residuals, **b** Cook's distance, **c** leverage plot vs. run, and **d** residuals vs. predicted plot

p-value = 0.8253. However, in the present result, the single effect of PEG became significant, this might be due to the effect of impregnated silica in the body of cellulose that produced a significant interaction with PEG. Moreover, several interactions between Si-cellulose and PEG were found to be significant with p-values of AB = 0.0196, $A^2 = 0.0136$, and $B^2 = 0.0209$, while insignificant effects were found in A2B = 0.7358 and $AB^2 = 0.1750$. The lack of fit was also insignificant with p-value = 0.5891, suggesting that the developed model can be reasonably accepted.

The R^2 of the developed model was extremely well fitted with a value of 0.9803, which is higher than the response on the cellulose and PEG model. It was also found that both adj-R^2 (0.9528) and pred-R^2 (0.8775) were in high precision of fit. The difference between both was 0.0753 which is below 0.2, suggesting that this model is adequate. To verify the quality of the model with the actual experimental data, the adequacy precision was found to be 19.65, which is acceptable because it is above the minimum value of 4. Additionally, the standard deviation of the model was measured to be 0.0096, which is relatively low and is acceptable, while the mean value was found to be 0.9463, and the CV% was 1.01%, indicating high data reliability. The ANOVA and adequacy parameter authenticates the developed SAC model with Si-cellulose and PEG as the material and suggests the model diagnostics.

The model diagnostics were evaluated to check whether errors of the developed model were either independently or identically distributed. The diagnostics analyses were employed using the normal plot of residuals, cook's distance, leverage plot, and residuals vs. predicted plot, as shown in Fig. 5. Based on Fig. 5a, the externally studentized residuals were well fitted on the normal plotline suggesting that the model is adequate. Furthermore, Fig. 5b shows the Cook's distance representing the effect of individual run that measures the changes in model parameters after replacing a particular actual run. Based on the results of cellulose and PEG in Fig. 2b, two experimental runs fell outside Cook's distance, while in the Si-cellulose and PEG sample, no experimental run fell outside the boundary. This shows that the accuracy of prediction for the Si-cellulose and PEG model is better than for cellulose and PEG. Figure 5c, d present the leverage and residuals vs. predicted plots that show the uniform distribution of the data on the developed response model. This indicates the good adequacy of the model to predict the response in the design space. Therefore, it was concluded that the model is adequate and can be used to navigate the response data.

3.2.3 Effects of impregnated silica on the characteristics of prepared silica-cellulose aerogel

Several characterizations were performed to further understand the physical and chemical characteristics of the fabricated silica-cellulose aerogel composite for the acoustic insulation materials. XRF analysis was carried out to present the silica (SiO_2) composition of several selected composites, i.e., the formulation at experimental run numbers 1, 3, and 11 with the constant composition of PEG and variation of cellulose concentration of 15, 29.14, and 0.86%w, respectively. Figure 6 represents the silica contents of different introduction amounts of cellulose. Initially, the silica content was increased with rising cellulose concentration up to a maximum value of 15%-w. At cellulose additions of 0.86, 15, and 29.14%-w, the silica contents were found to be 16, 86.7, and 9.7%, respectively. After achieving a maximum value at 15%, the trend of silica content decreased with an increase in cellulose concentration. This is presumably due to the increment in solution viscosity and density at higher concentrations of cellulose during the impregnation of silica using sodium silicate [54]. Hence, the penetration of silica to be embedded into the body of cellulose is reduced. The microstructure of the fabricated Si-cellulose aerogels can be further discussed with SEM results.

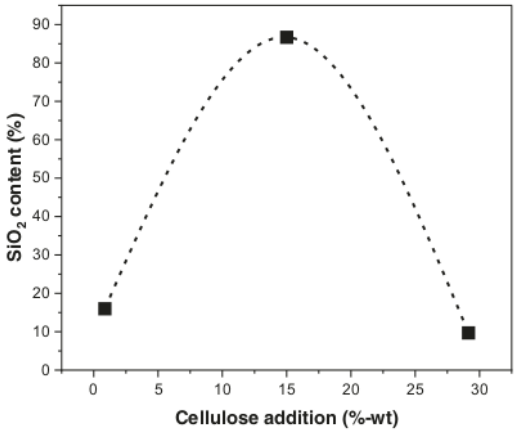

Fig. 6 XRF analysis results revealing the silica content of Si-cellulose aerogel for the additions of cellulose of 0.86, 15, and 29.14%w

SEM analysis was performed to reveal the surface microstructure of the fabricated Si-cellulose aerogel composites. In addition, the EDX analysis was also performed to clearly show the chemical composition of the generated SEM images. Figure 7a, b shows the SEM images and EDX results for the prepared Si-cellulose aerogel with cellulose addition of 15%-w and 0.86%-w, respectively. Based on the results, the generated composite with 15%-w of cellulose had a more compact structure than 0.86%. The micromorphology of the Si-cellulose composite with 0.86%w cellulose showed a highly porous structure that is not desirable for sound insulation due to its poor performance. The compact structure is presumably due to the

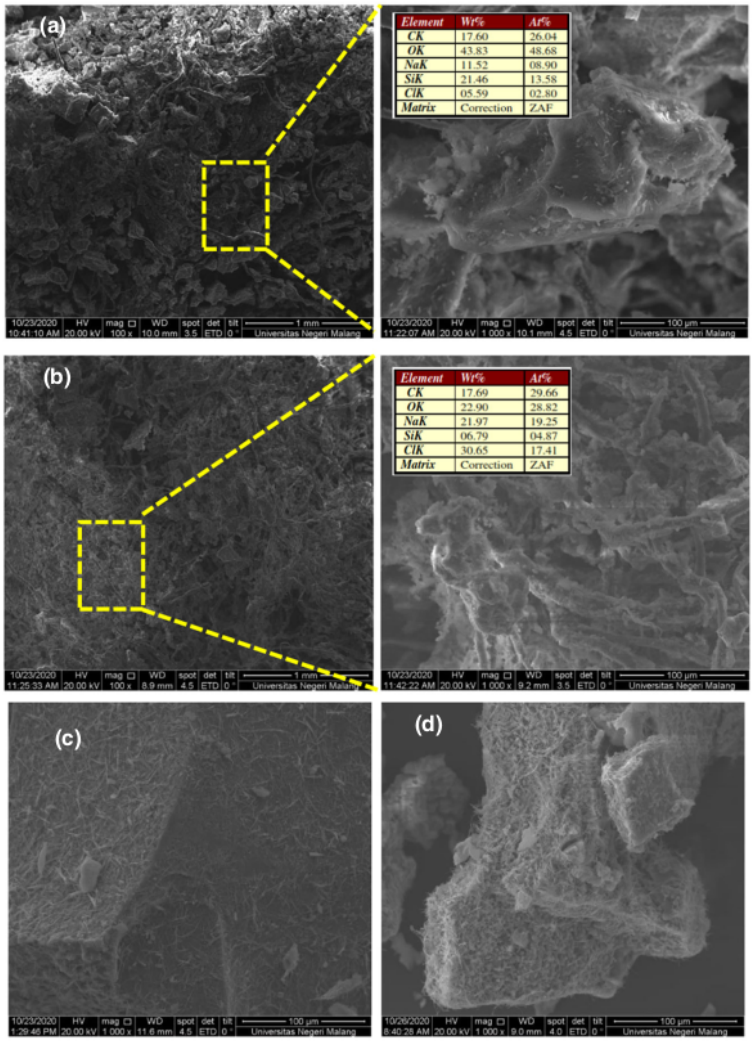

Fig. 7 SEM image for certain cellulose concentration in the product. **a** 15%-w with EDX result (Si-cellulose aerogel), **b** 0.86 %-w with EDX result (Si-cellulose aerogel), **c** cellulose aerogel, and **d** Si-cellulose

influence of cellulose concentration. A higher concentration can cause the formation of a denser layer in the body of the Si-cellulose composite [47]. According to the EDX results, the fabricated Si-cellulose aerogel with cellulose addition of 15%-w had a higher composition of silica namely 21.46% compared to cellulose addition of 0.86%-w which had 6.79%. The higher silica content in the composite is desirable because it can enhance the ability of sound absorption. Figure 7c, d show the comparisons of the cellulose and Si-cellulose aerogel micromorphology. As demonstrated in Fig. 7c, the cellulose surface is uniformly smooth, while (d) shows that the silica particles are stuck on the surface and held together due to the fiber structures of the cellulose to generate a compact composite structure signaling that the synthesis of Si-cellulose was successful.

Moreover, the BET analysis was carried out to show the physical pore properties of the fabricated Si-cellulose composites. It was found that the addition of 0.86%-w cellulose produced a surface area of 38.9320 m^2/g, which is higher than the Si-cellulose composite with the addition of 15%-w of cellulose namely 35.6610 m^2/g. The adsorbed volume range of Si-cellulose with the addition of 0.86%-w cellulose was also higher than the addition of 15%w. This is because the porous structure of Si-cellulose with the addition of 0.86%-w cellulose produced more contact area which led to a higher surface area and adsorbed volume in agreement with the SEM

results. However, a composite with a porous structure is not desirable for sound insulation purposes. Therefore, the Si-composite with a compact structure shows a higher sound absorption ability.

To further analyze the chemical characteristics of the composites, the FTIR analysis was performed. Figure 8 shows the FTIR spectra for cellulose and Si-cellulose aerogel. Based on the results, the vibrations of O-H groups were found at a wavenumber of 3608 cm^{-1}, showing a broad peak which indicates the O-H groups of polysaccharides [55], while the sharp peak around 2876 cm^{-1} indicates the strain vibrations of C-H bonds in polysaccharides [55]. Furthermore, typical bands of cellulose were detected at a wavenumber of 1800–1000 cm^{-1}. Several peaks at 1763, 1346, and 1029 cm^{-1} that corresponds to C = C bonds, C-H stretch, and C = O bonds were also found [55]. The typical peaks of silica were recorded at a wavenumber of 800–450 cm^{-1}, while a tiny peak at 796 cm^{-1} was found for the Si-cellulose aerogel indicating stretching vibrations of Si-O-Si groups [56]. These FTIR results confirmed that the composite is a cellulose material and the impregnation of silica was successful. Based on the results, the proposed formation mechanism of Si-cellulose aerogel is represented in Fig. 9. It is similar to a previous study which applied sodium silicate precursor for Si-cellulose synthesis [57].

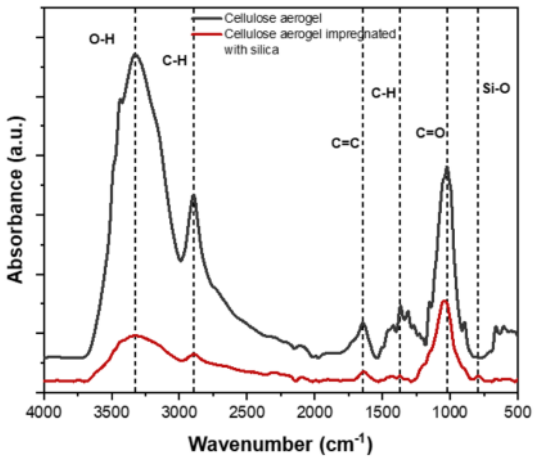

Fig. 8 FTIR spectra of cellulose aerogel (upper line) and Si-cellulose (bottom line) aerogel

To evaluate the thermal properties of the fabricated Si-cellulose composites, TGA and DSC analyses were performed. TGA analysis confirmed the weight loss characteristics at applied temperatures of 30–800 °C. Figure 10a–c show the TGA thermograms of Si-cellulose composite with the cellulose addition of 0.86, 15, and 29.14%w. The total weight losses of all three samples were 75.03, 45.89, and 91.23% respectively. Furthermore, the thermal behavior was highly influenced by the silica content in the composite. As stated earlier, based on XRF results, the silica contents were 16, 86.7, and 9.7% for Si-cellulose composites with cellulose addition of 0.86, 15, and 29.14% w, respectively. The thermal stability of the composite increased with higher silica content. This is presumably due to the high amount of silica that contributes to increasing the performance of the Si-composite. As shown in Fig. 10d, the DSC analysis shows that the first change in the thermal behavior was detected at temperatures of 47, 95, and 151 °C for the Si-cellulose composite with cellulose addition of 0.86, 15, and 29.14%-w, respectively. The cellulose addition of 29.14%-w and 15%-w produced the lowest and highest thermal stability, respectively. This shows that the thermal behavior of the prepared Si-cellulose composite is highly influenced by the silica content, the higher the

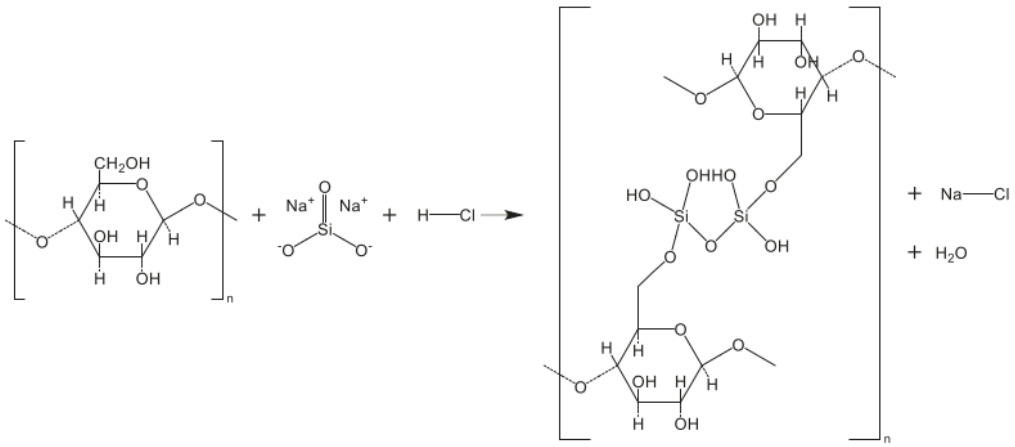

Fig. 9 Formation mechanism of Si-cellulose aerogel

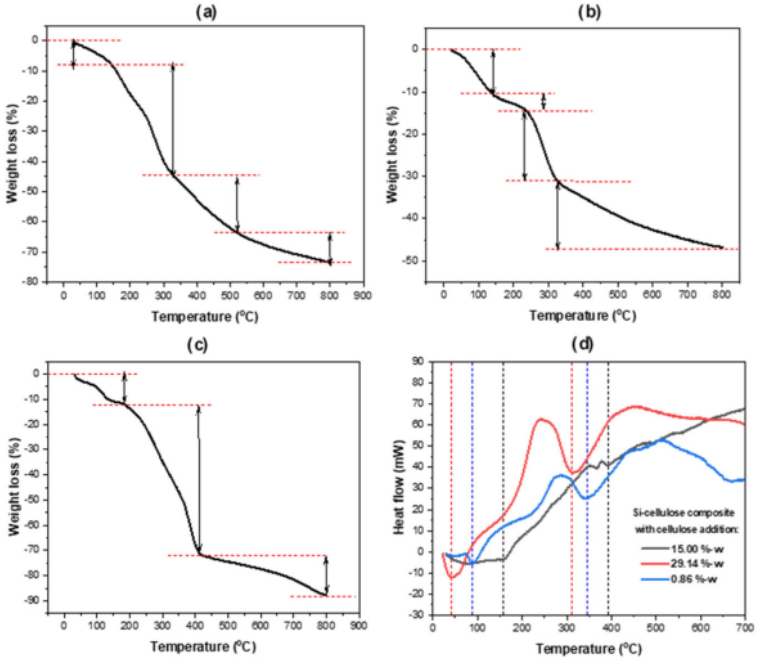

Fig. 10 TGA analysis results of Si-cellulose composites with certain cellulose concentration. **a** 0.86%-w, **b** 15%-w, **c** 29.14%-w, and **d** DSC analysis results

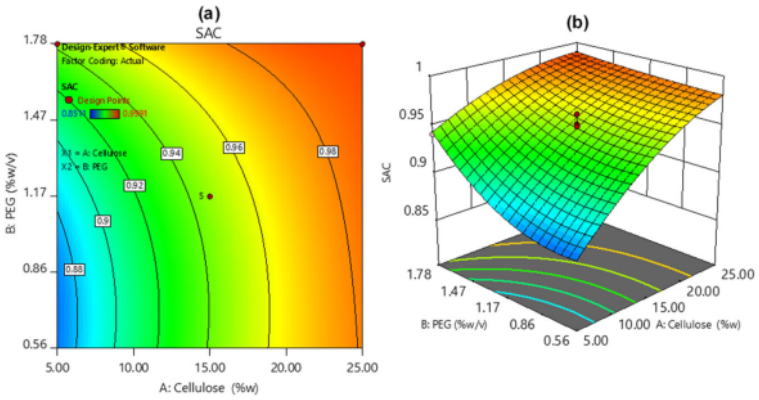

Fig. 11 Evaluation of the standard error of design for the experimental design for the Si-cellulose aerogel. **a** Contour plot of the standard error of design and **b** surface plot of the standard error of design

content, the higher the thermal stability. These results are in agreement with the TGA data previously discussed. Based on the analyses, it was concluded that the impregnation of silica into the cellulose was successful. The process produced a desirable structure, high sound absorption performance, as well as has high thermal stability that is suitable for the acoustic insulation material.

3.2.4 Response surface analysis and optimization

The impacts of Si-cellulose and PEG on SAC values were evaluated by analyzing the response generated from the regression equation as demonstrated by the contour (Fig. 11a) and surface plot (Fig. 11b). The SAC values ranged from 0.8511 to 0.9991, the lower the concentrations of Si-cellulose and PEG, the lower the SAC value and vice versa as shown in Fig. 11. The changing concentrations of Si-cellulose and PEG significantly influenced the sound absorption ability of the fabricated composite. The results showed that both played the same dominant role. This was quite different from the response surface of cellulose and PEG, where cellulose plays a more dominant role in generating the sound absorption ability of the composite.

The information from response surface plots is essential to perform an optimization. The primary goal was to find the formulation that generated the highest SAC value.

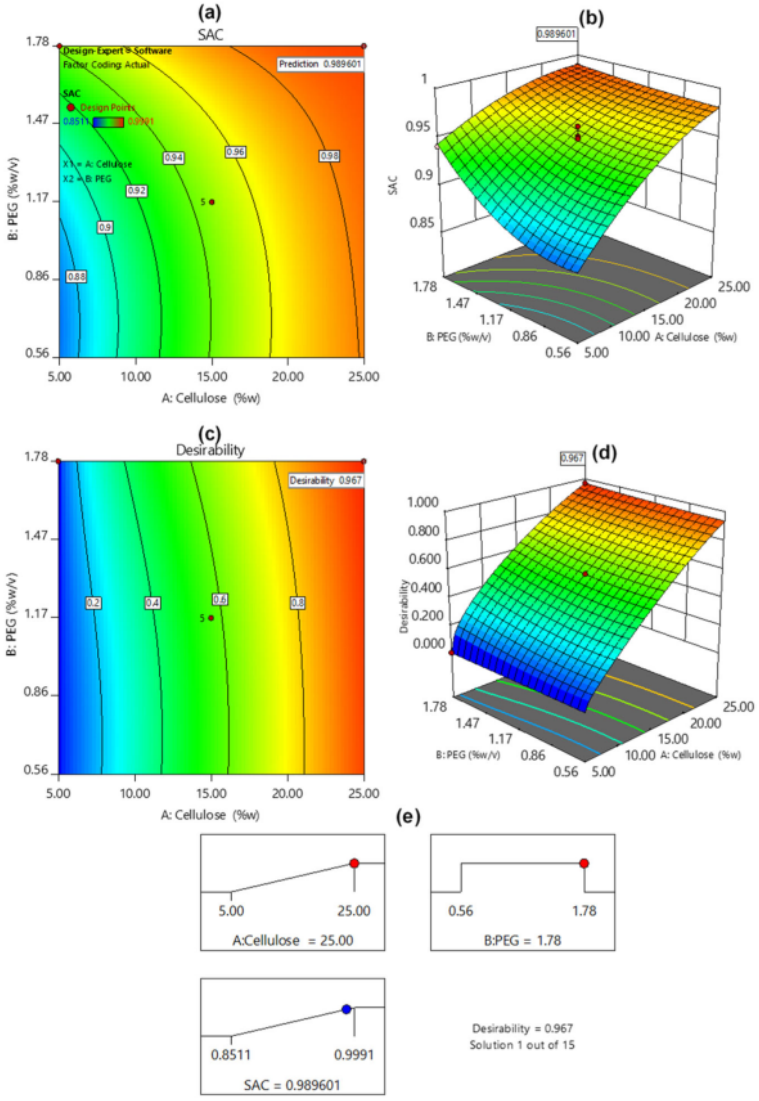

Fig. 12 Plotting of the optimization result for the Si-cellulose aerogel. **a** Contour plot of predicted SAC, **b** surface plot of predicted SAC, **c** contour plot of estimated desirability, **d** surface plot of estimated desirability, and **e** Ramp diagram

Table 5 The optimization summary of the formulation of Si-cellulose aerogel

Component	Optimized composition	Predicted SAC	Observed SAC	Difference (%)
Cellulose (%-w)	25	0.9896	0.9992	0.96
PEG (%-w/v)	1.78			
Desirability	0.967			

Hence, the optimization was targeted to (i) maximize the SAC value, (ii) maximize the utilization of Si-cellulose, and (iii) select the PEG concentration in range. It was conducted by applying the desirability parameter, which considered all targets into a single desirability score. Figure 12a shows the contour plot, while Fig. 12b represents the surface plot of the predicted SAC value produced by the optimization. Furthermore, Fig. 12c presents the

contour plot, 12(d) shows the surface plot of the desirability score, while Fig. 12e demonstrates the Ramp's diagrams of the optimization result showing that at 25%-w of cellulose and 1.78%-w/v of PEG, a SAC value of 0.9896 was obtained with a desirability score of 0.967. This result is similar to the previous optimization on cellulose and PEG, but the prediction of SAC value on Si-cellulose and PEG was slightly higher. The summary of optimization is shown in Table 5. Based on the validation experiment, the observed SAC for the optimized formulation was 0.9992, with a difference in the percentage of 0.96%, suggesting the extraordinary precision of the model. Therefore, the Si-cellulose aerogel composite is a prominent material for acoustic insulation purposes.

4 Conclusion

This study explores the combination of cellulose derived from newspaper waste and silica from geothermal solid waste to produce the Si-cellulose aerogel as an enhanced sound insulation composite material. Cellulose was utilized as the matrix, while silica was applied as the impregnated particle to improve the mechanical strength, thermal stability, and sound absorption ability of the composite. Silica was impregnated to cellulose through the sol-gel method using sodium silicate with hydrochloric acid and then solidified using a freeze dryer to form Si-cellulose aerogel. To comprehensively investigate the best formulation and to evaluate the effect of variables on the fabricated aerogel, two datasets of central composite experimental design (CCD) with 13 runs were performed to generate the regression models with the independent variables of cellulose and polyethylene glycol (PEG) concentrations as well as sound absorption coefficient (SAC) as the response variable. The generated regression models were evaluated using RMSE, ANOVA, model adequacy, and diagnostics with the normal plot of residuals, Cook's distance, leverage, and predicted vs. residuals plot. The generated response surface plots suggest that the maximum SAC will be achieved by maximizing the cellulose composition. Based on XRF, EDX, SEM, BET, FTIR, TGA, and DSC, it was concluded that the embedded silica changed the physical, chemical, mechanical, and thermal stability of the fabricated composite to enhance the acoustic insulation performance. Furthermore, the optimum point for the aerogel namely at cellulose and PEG compositions of 25%-w and 1.78%-w/v produced the predicted maximum SAC of 0.9896 with a desirability score of 0.967. Based on the validation experiment result, the actual SAC was 0.9992 with a difference of 0.96%, indicating that the generated model can precisely predict the actual SAC value for utilizing Si-cellulose as an acoustic insulation material.

Acknowledgements The authors are grateful to the community of the Advanced Material Laboratory (AMaL), Department of Chemical Engineering, Diponegoro University for all support and discussion in the study.

Author Contributions SS: conceptualization, methodology, supervision, funding acquisition, resources, writing – original draft. FH: methodology, investigation, supervision. JI: investigation, software, formal analysis. DALK: investigation, software, formal analysis. FD: data curation, software, visualization, formal analysis, writing – review and editing.

Funding This study was financially supported by the Directorate General of Higher Education, the Ministry of Education, Culture, Research, and Technology of the Republic of Indonesia with grant number 257-68/UN7.6.1/PP/2020.

Compliance with ethical standards

Conflict of interest The authors declare no competing interests.

References

1. Apparicio P, Gelb J, Carrier M et al. (2018) Exposure to noise and air pollution by mode of transportation during rush hours in Montreal. J Transp Geogr 70:182–192. https://doi.org/10.1016/j.jtrangeo.2018.06.007
2. Daley A (2008) Exercise and depression: a review of reviews. J Clin Psychol Med Settings 15:140–147. https://doi.org/10.1007/s10880-008-9105-z
3. Monazzam MR, Karimi E, Shahbazi H, Shahidzadeh H (2021) Effect of cycling development as a non-motorized transport on reducing air and noise pollution-case study: Central districts of Tehran. Urban Clim 38:100887. https://doi.org/10.1016/j.uclim.2021.100887
4. Kusuma APW, Ekasiwi SNN, Arifianto D (2015) Application of acoustic material for facade to reduce noise impact in building located near from rail. J Arch 14:33. https://doi.org/10.12962/j2355262x.v14i1.a885
5. Gazzola C, Caverni S, Corigliano A (2021) From mechanics to acoustics: Critical assessment of a robust metamaterial for acoustic insulation application. Appl Acoust 183:108311. https://doi.org/10.1016/j.apacoust.2021.108311
6. Islam S, Bhat G (2019) Environmentally-friendly thermal and acoustic insulation materials from recycled textiles. J Environ Manag 251:109536. https://doi.org/10.1016/j.jenvman.2019.109536
7. Lin Q, Lin Q, Wang Y, Di G (2021) Sound insulation performance of sandwich structure compounded with a resonant acoustic metamaterial. Compos Struct 273:114312. https://doi.org/10.1016/j.compstruct.2021.114312
8. Aly NM, Seddeq HS, Elnagar K, Hamouda T (2021) Acoustic and thermal performance of sustainable fiber reinforced thermoplastic composite panels for insulation in buildings. J Build Eng 40:102747. https://doi.org/10.1016/j.jobe.2021.102747
9. Pérez G, Coma J, Barreneche C et al. (2016) Acoustic insulation capacity of Vertical Greenery Systems for buildings. Appl Acoust 110:218–226. https://doi.org/10.1016/j.apacoust.2016.03.040
10. Kim H, Hong J, Pyo S (2018) Acoustic characteristics of sound absorbable high performance concrete. Appl Acoust 138:171–178. https://doi.org/10.1016/j.apacoust.2018.04.002

11. Kusno A, Sakagami K, Okuzono T et al. (2019) A pilot study on the sound absorption characteristics of chicken feathers as an alternative sustainable acoustical material. Sustainability 11:1476. https://doi.org/10.3390/su11051476
12. del Rey R, Uris A, Alba J, Candelas P (2017) Characterization of sheep wool as a sustainable material for acoustic applications. Mater (Basel) 10:1277. https://doi.org/10.3390/ma10111277
13. Mazrouei-Sebdani Z, Begum H, Schoenwald S et al. (2021) A review on silica aerogel-based materials for acoustic applications. J Non Cryst Solids 562:120770. https://doi.org/10.1016/j.jnoncrysol.2021.120770
14. Tran DT, Nguyen ST, Do ND et al. (2020) Green aerogels from rice straw for thermal, acoustic insulation and oil spill cleaning applications. Mater Chem Phys 253:123363. https://doi.org/10.1016/j.matchemphys.2020.123363
15. Long L-Y, Weng Y-X, Wang Y-Z (2018) Cellulose aerogels: synthesis, applications, and prospects. Polym (Basel) 10:623. https://doi.org/10.3390/polym10060623
16. Melo RP, Rosa MP, da, Beck PH et al. (2021) Thermal, morphological and mechanical properties of composites based on polyamide 6 with cellulose, silica and their hybrids from rice husk. J Compos Mater 55:1811–1821. https://doi.org/10.1177/0021998320978290
17. Silva L, Panzera T, Velloso V et al. (2013) Statistical design of polymeric composites reinforced with banana fibres and silica microparticles. J Compos Mater 47:1199–1210. https://doi.org/10.1177/0021998312446499
18. Magdaleno-López C, Pérez-Bueno J, de J, Flores-Segura JC et al. (2019) A geopolymeric composite of non-calcined rice husks made of metakaolin/sol–gel silica. J Compos Mater 53:603–611. https://doi.org/10.1177/0021998318788145
19. Kayo C, Dente SMR, Aoki-Suzuki C et al. (2019) Environmental impact assessment of wood use in Japan through 2050 using material flow analysis and life cycle assessment. J Ind Ecol 23:635–648. https://doi.org/10.1111/jiec.12766
20. Felgueiras C, Azoia NG, Gonçalves C et al. (2021) Trends on the cellulose-based textiles: raw materials and technologies. Front Bioeng Biotechnol 9: https://doi.org/10.3389/fbioe.2021.608826
21. Moreno YP, da Silva WL, Stedile FC et al. (2021) Micro and nanodomains on structured silica/titania photocatalysts surface evaluated in RhB degradation: Effect of structural properties on catalytic efficiency. Appl Surf Sci Adv 3:100055. https://doi.org/10.1016/j.apsadv.2021.100055
22. da Silva WL, Lansarin MA, Stedile FC, dos Santos JHZ (2014) The potential of chemical industrial and academic wastes as a source of supported photocatalysts. J Mol Catal A Chem 393:125–133. https://doi.org/10.1016/j.molcata.2014.05.040
23. Muraro PCL, Mortari SR, Vizzotto BS et al. (2020) Iron oxide nanocatalyst with titanium and silver nanoparticles: Synthesis, characterization and photocatalytic activity on the degradation of Rhodamine B dye. Sci Rep. 10:3055. https://doi.org/10.1038/s41598-020-59987-0
24. Chen W, Hu S, Cao H et al. (2019) Review on research process of sound reduction materials. IOP Conf Ser Mater Sci Eng 612:052062. https://doi.org/10.1088/1757-899X/612/5/052062
25. Zhang G, Xu B, Zhang K et al. (2020) Research on a noise reduction method based on multi-resolution singular value decomposition. Appl Sci 10:1409. https://doi.org/10.3390/app10041409
26. Nguyen ST, Feng J, Ng SK et al. (2014) Advanced thermal insulation and absorption properties of recycled cellulose aerogels. Colloids Surf A Physicochem Eng Asp 445:128–134. https://doi.org/10.1016/j.colsurfa.2014.01.015
27. Gurinov AA, Mauder D, Akcakayiran D et al. (2012) Does water affect the acidity of surfaces? The proton-donating ability of silanol and carboxylic acid groups at mesoporous silica. ChemPhysChem 13:2282–2285. https://doi.org/10.1002/cphc.201200204
28. Silviana S, Darmawan A, Dalanta F et al. (2021) Superhydrophobic coating derived from geothermal silica to enhance material durability of bamboo using hexadimethylsilazane (HMDS) and trimethylchlorosilane (TMCS). Mater (Basel) 14:530. https://doi.org/10.3390/ma14030530
29. Silviana S, Bayu WJ (2018) Silicon conversion from bamboo leaf silica by magnesiothermic reduction for development of li-ion baterry anode. MATEC Web Conf 156:05021. https://doi.org/10.1051/matecconf/201815605021
30. Permatasari N, Sucahya TN, Dani Nandiyanto AB (2016) Review: agricultural wastes as a source of silica material. Indones J Sci Technol 1:82. https://doi.org/10.17509/ijost.v1i1.8619
31. Silviana S, Sanyoto GJ, Darmawan A, Sutanto H (2020) Geothermal silica waste as sustainable amorphous silica source for the synthesis of silica xerogels. Rasayan J Chem 13:1692–1700. https://doi.org/10.31788/RJC.2020.1335701
32. Silviana S, Darmawan A, Subagio A, Dalanta F (2020) Statistical approaching for superhydrophobic coating preparation using silica derived from geothermal solid waste. ASEAN J Chem Eng 19:91. https://doi.org/10.22146/ajche.51178
33. Silviana S, Ma'ruf A (2020) Silicon preparation derived from geothermal silica by reduction using magnesium. Int J Emerg Trends Eng Res 8:4861–4866. https://doi.org/10.30534/ijeter/2020/126882020
34. Pumomo A, Dalanta F, Oktaviani AD, Silviana S (2018) Superhydrophobic coatings and self-cleaning through the use of geothermal scaling silica in improvement of material resistance. AIP Conf Proc 2026:020077. https://doi.org/10.1063/1.5065037
35. Villarias JA, Yorro MLH, Galvan MIKN, Diaz LJL (2017) High purity silica nanoparticles from geothermal waste brine as reinforcing filler in rubber composite material. Mater Sci Forum 894:104–108
36. Silviana S, Anggoro DD, Salsabila CA, Aprilio K (2021) Utilization of geothermal waste as a silica adsorbent for biodiesel purification. Korean J Chem Eng 38:2091–2105. https://doi.org/10.1007/s11814-021-0827-z
37. Silviana S, Jethro Sanyoto G, Darmawan A (2021) Preparation of geothermal silica glass coating film through multi-factor optimization. J Teknol 83:41–49. https://doi.org/10.11113/jurnalteknologi.v83.16377
38. Silviana S, Ma'ruf A (2020) Silicon preparation derived from geothermal silica by reduction using magnesium. Int J Emerg Trends Eng Res 8:4861–4866. https://doi.org/10.30534/ijeter/2020/126882020
39. Silviana S, Dalanta F, Sanyoto GJ (2021) Utilization of bamboo leaf silica as a superhydrophobic coating using trimethylchlorosilane as a surface modification agent. J Phys Conf Ser 1943:012180. https://doi.org/10.1088/1742-6596/1943/1/012180
40. Silviana S, Noorpasha A, Rahman MM (2020) Preliminary study of chitosan coating silica derived from geotermal solid waste. Civ Eng Arch 8:281–288. https://doi.org/10.13189/cea.2020.080311
41. Silviana S, Darmawan A, Janitra AA (2020) Synthesized silica mesoporous from silica geothermal assisted with CTAB and modified by APTMS. Int J Emerg Trends Eng Res 8:4854–4860. https://doi.org/10.30534/ijeter/2020/125882020
42. Silviana S, Purbasari A, Siregar A, Rochayati AF, Papra T (2020) Synthesis of mesoporous silica derived from geothermal waste with cetyl trimethyl ammonium bromide (CTAB) surfactant as drug delivery carrier. AIP Conf Proc 2296:020083. https://doi.org/10.1063/5.0030487
43. Silviana S, Rambe INH, Sudrajat H, Zidan MA (2019) Statistical approaching of sol-gel process in preparation of silica aerogel derived from geothermal silica by several acids. AIP Conf Proc 2202:020069. https://doi.org/10.1063/1.5141682

44. Imam MA, Jeelani S, Rangari VK (2019) Thermal decomposition and mechanical characterization of poly (lactic acid) and potato starch blend reinforced with biowaste SiO_2. J Compos Mater 53:2315–2334. https://doi.org/10.1177/0021998319826377
45. Cruz E, Radler M, Perello M, Savastano Jr H (2021) Fiber cement boards modified with styrene-acrylic copolymer: An approach to address dimensional stability and cellulose fiber preservation. J Compos Mater 55:437–452. https://doi.org/10.1177/0021998320951224
46. Sedighi Gilani M, Boone MN, Fife JL et al. (2016) Structure of cellulose -silica hybrid aerogel at sub-micron scale, studied by synchrotron X-ray tomographic microscopy. Compos Sci Technol 124:71–80. https://doi.org/10.1016/j.compscitech.2016.01.013
47. Feng J, Le D, Nguyen ST et al. (2016) Silica-cellulose hybrid aerogels for thermal and acoustic insulation applications. Colloids Surf A Physicochem Eng Asp 506:298–305. https://doi.org/10.1016/j.colsurfa.2016.06.052
48. Affandi S, Setyawan H, Winardi S et al. (2009) A facile method for production of high-purity silica xerogels from bagasse ash. Adv Powder Technol 20:468–472. https://doi.org/10.1016/j.apt.2009.03.008
49. Srasri K, Thongroj M, Chaijiraaree P et al. (2018) Recovery potential of cellulose fiber from newspaper waste: An approach on magnetic cellulose aerogel for dye adsorption material. Int J Biol Macromol 119:662–668. https://doi.org/10.1016/j.ijbiomac.2018.07.123
50. Yan L, Gao Z (2008) Dissolving of cellulose in PEG/NaOH aqueous solution. Cellulose 15:789–796. https://doi.org/10.1007/s10570-008-9233-5
51. Zainulabidin M, Rani M, Nezere N, Tobi A (2014) Optimum sound absorption by materials fraction combination. Int J Mech Mechatron Eng 14:118–121
52. Venkatesan M, Zaib Q, Shah IH, Park HS (2019) Optimum utilization of waste foundry sand and fly ash for geopolymer concrete synthesis using D-optimal mixture design of experiments. Resour Conserv Recycl 148:114–123. https://doi.org/10.1016/j.resconrec.2019.05.008
53. Li Z, Lu D, Gao X (2021) Optimization of mixture proportions by statistical experimental design using response surface method - A review. J Build Eng 36:102101. https://doi.org/10.1016/j.jobe.2020.102101
54. Oh KW, Kim DK, Kim SH (2009) Ultra-porous flexible PET/Aerogel blanket for sound absorption and thermal insulation. Fibers Polym 10:731–737. https://doi.org/10.1007/s12221-010-0731-3
55. Hospodarova V, Singovszka E, Stevulova N (2018) Characterization of cellulosic fibers by FTIR spectroscopy for their further implementation to building materials. Am J Anal Chem 09:303–310. https://doi.org/10.4236/ajac.2018.96023
56. Ashori A, Sheykhnazari S, Tabarsa T et al. (2012) Bacterial cellulose/silica nanocomposites: Preparation and characterization. Carbohydr Polym 90:413–418. https://doi.org/10.1016/j.carbpol.2012.05.060
57. Chen YX, Sepahvand S, Gauvin F et al. (2021) One-pot synthesis of monolithic silica-cellulose aerogel applying a sustainable sodium silicate precursor. Constr Build Mater 293:123289. https://doi.org/10.1016/j.conbuildmat.2021.123289

Terms and Conditions

Springer Nature journal content, brought to you courtesy of Springer Nature Customer Service Center GmbH ("Springer Nature").

Springer Nature supports a reasonable amount of sharing of research papers by authors, subscribers and authorised users ("Users"), for small-scale personal, non-commercial use provided that all copyright, trade and service marks and other proprietary notices are maintained. By accessing, sharing, receiving or otherwise using the Springer Nature journal content you agree to these terms of use ("Terms"). For these purposes, Springer Nature considers academic use (by researchers and students) to be non-commercial.

These Terms are supplementary and will apply in addition to any applicable website terms and conditions, a relevant site licence or a personal subscription. These Terms will prevail over any conflict or ambiguity with regards to the relevant terms, a site licence or a personal subscription (to the extent of the conflict or ambiguity only). For Creative Commons-licensed articles, the terms of the Creative Commons license used will apply.

We collect and use personal data to provide access to the Springer Nature journal content. We may also use these personal data internally within ResearchGate and Springer Nature and as agreed share it, in an anonymised way, for purposes of tracking, analysis and reporting. We will not otherwise disclose your personal data outside the ResearchGate or the Springer Nature group of companies unless we have your permission as detailed in the Privacy Policy.

While Users may use the Springer Nature journal content for small scale, personal non-commercial use, it is important to note that Users may not:

1. use such content for the purpose of providing other users with access on a regular or large scale basis or as a means to circumvent access control;
2. use such content where to do so would be considered a criminal or statutory offence in any jurisdiction, or gives rise to civil liability, or is otherwise unlawful;
3. falsely or misleadingly imply or suggest endorsement, approval , sponsorship, or association unless explicitly agreed to by Springer Nature in writing;
4. use bots or other automated methods to access the content or redirect messages
5. override any security feature or exclusionary protocol; or
6. share the content in order to create substitute for Springer Nature products or services or a systematic database of Springer Nature journal content.

In line with the restriction against commercial use, Springer Nature does not permit the creation of a product or service that creates revenue, royalties, rent or income from our content or its inclusion as part of a paid for service or for other commercial gain. Springer Nature journal content cannot be used for inter-library loans and librarians may not upload Springer Nature journal content on a large scale into their, or any other, institutional repository.

These terms of use are reviewed regularly and may be amended at any time. Springer Nature is not obligated to publish any information or content on this website and may remove it or features or functionality at our sole discretion, at any time with or without notice. Springer Nature may revoke this licence to you at any time and remove access to any copies of the Springer Nature journal content which have been saved.

To the fullest extent permitted by law, Springer Nature makes no warranties, representations or guarantees to Users, either express or implied with respect to the Springer nature journal content and all parties disclaim and waive any implied warranties or warranties imposed by law, including merchantability or fitness for any particular purpose.

Please note that these rights do not automatically extend to content, data or other material published by Springer Nature that may be licensed from third parties.

If you would like to use or distribute our Springer Nature journal content to a wider audience or on a regular basis or in any other manner not expressly permitted by these Terms, please contact Springer Nature at

onlineservice@springernature.com

Optimizing the environmentally friendly silica-cellulose aerogel composite for acoustic insulation material derived from newspaper and geothermal solid waste using a central composite design

ORIGINALITY REPORT

16%	8%	14%	3%
SIMILARITY INDEX	INTERNET SOURCES	PUBLICATIONS	STUDENT PAPERS

PRIMARY SOURCES

1	Mayandi Venkatesan, Qammer Zaib, Izhar Hussain Shah, Hung Suck Park. "Optimum utilization of waste foundry sand and fly ash for geopolymer concrete synthesis using D-optimal mixture design of experiments", Resources, Conservation and Recycling, 2019 Publication	2%
2	Febio Dalanta, Tutuk Djoko Kusworo, Nita Aryanti, Nur Hidayati Othman. "Optimization of AC/TiO2/CeO2 composite formulation for petroleum refinery wastewater treatment via simultaneous adsorption-photocatalytic process using D-optimal mixture experimental design", Journal of Environmental Chemical Engineering, 2021 Publication	2%
3	Bin Yuan, Jinming Zhang, Qinyong Mi, Jian Yu, Rui Song, Jun Zhang. "Transparent Cellulose–Silica Composite Aerogels with Excellent	1%

	Flame Retardancy via an in Situ Sol–Gel Process", ACS Sustainable Chemistry & Engineering, 2017 Publication	
4	S. Silviana, Atikah A. Janitra, Afriza N. Sa'adah, Febio Dalanta. "Synthesis of Aminopropyl-Functionalized Mesoporous Silica Derived from Geothermal Silica for an Effective Slow-Release Urea Carrier", Industrial & Engineering Chemistry Research, 2022 Publication	1 %
5	www.mdpi.com Internet Source	1 %
6	Submitted to Leiden University Student Paper	1 %
7	www.nature.com Internet Source	<1 %
8	"Cellulose-Based Superabsorbent Hydrogels", Springer Science and Business Media LLC, 2019 Publication	<1 %
9	coek.info Internet Source	<1 %
10	ifory.id Internet Source	<1 %
11	www.frontiersin.org Internet Source	

		<1%
12	Xiuhong Li, Yujie Peng, Youqi He, Chupeng Zhang, Daode Zhang, Yong Liu. "Research Progress on Sound Absorption of Electrospun Fibrous Composite Materials", Nanomaterials, 2022 Publication	<1%
13	dokumen.pub Internet Source	<1%
14	"Green Composites", Springer Science and Business Media LLC, 2021 Publication	<1%
15	Jingduo Feng, Duyen Le, Son T. Nguyen, Victor Tan Chin Nien, Daniel Jewell, Hai M. Duong. "Silicacellulose hybrid aerogels for thermal and acoustic insulation applications", Colloids and Surfaces A: Physicochemical and Engineering Aspects, 2016 Publication	<1%
16	Pragya Gupta, Balwant Singh, Ashish K. Agrawal, Pradip K. Maji. "Low density and high strength nanofibrillated cellulose aerogel for thermal insulation application", Materials & Design, 2018 Publication	<1%

17	Jatin Sood, Bharti Sapra, Ashok K. Tiwary. "Microemulsion Transdermal Formulation for Simultaneous Delivery of Valsartan and Nifedipine: Formulation by Design", AAPS PharmSciTech, 2016 Publication	<1 %
18	medium.com Internet Source	<1 %
19	eprints.uthm.edu.my Internet Source	<1 %
20	Xin Chen, Feng Yu, Jing Yu, Shuaikang Li. "Experimental optimization of industrial waste-based soil hardening agent: Combining D-optimal design with genetic algorithm", Journal of Building Engineering, 2023 Publication	<1 %
21	daneshyari.com Internet Source	<1 %
22	Silviana Silviana, Amar Ma'ruf, Febio Dalanta. "Silicone for Lithium-Ion Battery Anode Derived from Geothermal Waste Silica through Magnesiothermic Reduction and Double Stages in Acid Leaching", Defect and Diffusion Forum, 2022 Publication	<1 %
23	Tong Lu, Zhen-hua Dan, Tian-jing Li, Guo-qing Dai, Yang-yang Sun, Yan-hua Guo, Kai Li, Dan-	<1 %

qing Yi, Hui Chang, Lian Zhou. "Flow softening and microstructural evolution of near β titanium alloy Ti-35421 during hot compression deformation in the α+β region", Journal of Materials Research and Technology, 2022
Publication

24	Submitted to Universitas Diponegoro Student Paper	<1 %
25	Y.X. Chen, S. Sepahvand, F. Gauvin, K. Schollbach, H.J.H Brouwers, Qingliang Yu. "One-pot synthesis of monolithic silica-cellulose aerogel applying a sustainable sodium silicate precursor", Construction and Building Materials, 2021 Publication	<1 %
26	Zhongwang Liu, Zhansheng Wu, Fei Tian, Xiaochen Liu, Tao Li, Yanhui He, Beibei Li, Ziyan Zhang, Bing Yu. "Phosphate-solubilizing microorganisms regulate the release and transformation of phosphorus in biochar-based slow-release fertilizer", Science of The Total Environment, 2023 Publication	<1 %
27	Tutuk Djoko Kusworo, Andri Cahyo Kumoro, Nita Aryanti, Tonni Agustiono Kurniawan, Febio Dalanta, Nur Hashimah Alias. "Photocatalytic polysulfone membrane	<1 %

	incorporated by ZnO-MnO2@SiO2 composite under UV light irradiation for the reliable treatment of natural rubber-laden wastewater", Chemical Engineering Journal, 2023 Publication	
28	openaccess.city.ac.uk Internet Source	<1 %
29	vdocument.in Internet Source	<1 %
30	www.idexlab.com Internet Source	<1 %
31	www.freepatentsonline.com Internet Source	<1 %
32	doc-pak.undip.ac.id Internet Source	<1 %
33	nstda.or.th Internet Source	<1 %
34	www.rasayanjournal.co.in Internet Source	<1 %
35	www.science.gov Internet Source	<1 %
36	Hai M. Duong, Nathaniel R.B. Ling, Quoc B. Thai, Duyen K. Le, Phuc T.T. Nguyen, Xue Yang Goh, Nhan Phan-Thien. "A novel aerogel from	<1 %

thermal power plant waste for thermal and acoustic insulation applications", Waste Management, 2021
Publication

37	article.sapub.org Internet Source	<1 %
38	journals.utm.my Internet Source	<1 %
39	www.gjesm.net Internet Source	<1 %
40	www.warse.org Internet Source	<1 %
41	"Earthquake Geotechnics", Springer Science and Business Media LLC, 2022 Publication	<1 %
42	Adem Yildirim, Tural Khudiyev, Bihter Daglar, Hulya Budunoglu, Ali K. Okyay, Mehmet Bayindir. "Superhydrophobic and Omnidirectional Antireflective Surfaces from Nanostructured Ormosil Colloids", ACS Applied Materials & Interfaces, 2013 Publication	<1 %
43	Congqi Luan, Mei Zhou, Tongtong Zhou, Jinbang Wang, Lianwang Yuan, Kai Zhang, Zunchao Ren, Yongyi Liu, Zonghui Zhou. "Optimizing the Design Proportion of High-Performance Concrete via Using Response	<1 %

Surface Method", Iranian Journal of Science and Technology, Transactions of Civil Engineering, 2022
Publication

---

44 Ebru Kurtulbaş, Raneen Albarri, Mehmet Torun, Selin Şahin. "Encapsulation of Moringa oleifera leaf extract in chitosan-coated alginate microbeads produced by ionic gelation", Food Bioscience, 2022 <1%
Publication

---

45 Gowthami Palanisamy, T. Sadhasivam, Won-Shik Park, Shin Tae Bae, Sung-Hee Roh, Ho-Young Jung. "Tuning the Ion Selectivity and Chemical Stability of a Biocellulose Membrane by PFSA Ionomer Reinforcement for Vanadium Redox Flow Battery Applications", ACS Sustainable Chemistry & Engineering, 2020 <1%
Publication

---

46 Jian Li, Yun Lu, Dongjiang Yang, Qingfeng Sun, Yixing Liu, Huijun Zhao. "Lignocellulose Aerogel from Wood-Ionic Liquid Solution (1-Allyl-3-methylimidazolium Chloride) under Freezing and Thawing Conditions", Biomacromolecules, 2011 <1%
Publication

---

47 Tatjana Rijavec. "Silica aerogel based high thermal insulation materials", Elsevier BV, <1%

	2023 Publication	
48	Xu Xu, Fuhao Dong, Xinxin Yang, He Liu, Lizhen Guo, Yuehan Qian, Aiting Wang, Shifa Wang, Jinyue Luo. "Preparation and Characterization of Cellulose Grafted with Epoxidized Soybean Oil Aerogels for Oil-Absorbing Materials", Journal of Agricultural and Food Chemistry, 2019 Publication	<1 %
49	accedacris.ulpgc.es Internet Source	<1 %
50	agronomy.emu.ee Internet Source	<1 %
51	catalog.lib.kyushu-u.ac.jp Internet Source	<1 %
52	ebin.pub Internet Source	<1 %
53	garuda.kemdikbud.go.id Internet Source	<1 %
54	hal.archives-ouvertes.fr Internet Source	<1 %
55	oak.ulsan.ac.kr Internet Source	<1 %
56	pubag.nal.usda.gov Internet Source	<1 %

57	ris.cdu.edu.au Internet Source	<1 %
58	www.deswater.com Internet Source	<1 %
59	www.scielo.br Internet Source	<1 %
60	www.scribd.com Internet Source	<1 %
61	Zhiping Li, Dagang Lu, Xiaojian Gao. "Optimization of mixture proportions by statistical experimental design using response surface method - A review", Journal of Building Engineering, 2021 Publication	<1 %
62	Lin-Yu Long, Yun-Xuan Weng, Yu-Zhong Wang. "Cellulose Aerogels: Synthesis, Applications, and Prospects", Polymers, 2018 Publication	<1 %
63	Mathibela E. Aphane, Frédéric J. Doucet, Richard A. Kruger, Leslie Petrik, Elizabet M. van der Merwe. "Preparation of Sodium Silicate Solutions and Silica Nanoparticles from South African Coal Fly Ash", Waste and Biomass Valorization, 2019 Publication	<1 %

64	Rubén Maderuelo-Sanz, Francisco José García-Cobos, Francisco José Sánchez-Delgado, María Isabel Mota-López et al. "Mechanical, thermal and acoustical evaluation of biocomposites made of agricultural waste for ceiling tiles", Applied Acoustics, 2022 Publication	<1 %
65	S Silviana, A N Sa'adah, R P Deastuti, N C Ramadhani et al. "Synthesis of silica-cellulose aerogel derived from bagasse through impregnation and ambient pressure drying methods as thermal insulator", IOP Conference Series: Earth and Environmental Science, 2022 Publication	<1 %

Exclude quotes	On	Exclude matches	Off
Exclude bibliography	On		

Optimizing the environmentally friendly silica-cellulose aerogel composite for acoustic insulation material derived from newspaper and geothermal solid waste using a central composite design

GRADEMARK REPORT

FINAL GRADE

/0

GENERAL COMMENTS

Instructor

PAGE 1

PAGE 2

PAGE 3

PAGE 4

PAGE 5

PAGE 6

PAGE 7

PAGE 8

PAGE 9

PAGE 10

PAGE 11

PAGE 12

PAGE 13

PAGE 14

PAGE 15

PAGE 16

PAGE 17

PAGE 18